ELSEVIER

Thermochimica Acta 348 (2000) 181–190

thermochimica acta

www.elsevier.com/locate/tca

Heat capacity by multi-frequencies sawtooth modulation☆

B. Wunderlich[a,*], R. Androsch[a,1], M. Pyda[a], Y.K. Kwon[b]

[a]*Department of Chemistry, The University of Tennessee, Knoxville, TN 37996-1600, USA*
[b]*Oak Ridge National Laboratory, Chemical and Analytical Sciences Division, Oak Ridge, TN 37831-6197, USA*

Received 27 September 1999; received in revised form 19 November 1999; accepted 2 December 1999

Abstract

In this paper a simple method is proposed to carry out temperature-modulated calorimetry with multiple frequencies. The method is based on modulation with a complex sawtooth. The harmonics of the Fourier series of the measured heat-flow rate and temperature are used to extract data pertaining to the frequencies of the 1st, 3rd, 5th, 7th and 9th harmonic. The complex sawtooth produces similar modulation amplitudes of the temperature of the first four harmonics. In temperature-modulated differential scanning calorimetry with a period of less than about 150 s, corrections by extrapolation to zero frequency are commonly needed. With the proposed method, these extrapolations can be done in a single experiment. Difficulties of baseline subtraction and other possible instrumentation and software problems are discussed. © 2000 Elsevier Science B.V. All rights reserved.

Keywords: Heat capacity; Temperature-modulated differential scanning calorimetry (TMDSC); Fourier transformation; Higher harmonics; Sawtooth modulation

1. Introduction

Heat capacity can be determined by a number of calorimetric techniques. Standard differential scanning calorimetry (DSC) has gained increasing popularity over the years because of its large temperature range from 10^2 to 10^3 K, and because of its ease of operation. The method requires the measurement of the differential heat-flow rate ΔHF into a sample and a reference calorimeter as response to a rate of temperature change which is forced by the heating program. The programmed temperature is a linear ramp over a rather large temperature interval (typically 50–100 K) with a heating rate of 5–40 K min^{-1} [1].

With the invention and development of temperature-modulated differential scanning calorimetry (TMDSC) [2–4] it became possible to provide data on the frequency-dependence of the heat capacity, as it is observed, e.g., in the glass-transition region [5]. The programmed temperature for TMDSC is produced by superposition of a constant, average heating rate $\langle q \rangle$, (typically 0.5–5.0 K) and a temperature-modulation

☆The submitted paper has been authored by a contractor of the US Government under the contract No. DE-AC05-96OR22464. Accordingly, the US Government retains a non-exclusive, royalty-free license to publish, or reproduce the published form of this contribution, or allow others to do so, for US Government purposes.

* Corresponding author. Tel.: +1-423-974-0652; fax: +1-423-974-3419.

E-mail address: athas@utk.edu (B. Wunderlich)

[1] Present address: Martin-Luther-University, Halle-Wittenberg, Institute of Materials Technology, Geusaer Str., 06217 Merseburg, Germany.

0040-6031/00/$ – see front matter © 2000 Elsevier Science B.V. All rights reserved.
PII: S0040-6031(99)00455-4

with a frequency ω ($=2\pi/p$) with a period p of usually 30–60 s and a sample-temperature amplitude of 0.1–1.0 K. The common types of modulations are sinusoidal or sawtooth-like and the usual method of evaluation involves taking the ratio of the amplitudes of the first harmonics of the heat flow rate, A_{HF}, and the rate of change of the sample temperature, $A_{T_s} \times \omega$, to be multiplied with the needed correction factors for the chosen sample and instrument.

The advantage of TMDSC using modulation with a sawtooth is its ease of precise generation, but it was shown that for modulation periods of less than about 150 s, the measured heat capacity is less than its true value [6]. The data need to be extrapolated to zero frequency to derive the true heat capacity. By using the first and several of the higher harmonics of the sawtooth one can, however, determine this frequency-dependence of the experimental data in a single run [7].

A simultaneous use of several modulation frequencies was proposed already at the outset of TMDSC [2–4] but, as far as we are aware of, has not yet been routinely applied to TMDSC. The disadvantage of using the higher harmonics for calculation of the true heat capacity is the rapid decrease in amplitude of the higher harmonics as can be seen in Eq. (1), shown below. In the present paper we demonstrate that it is possible to produce a complex, centrosymmetric sawtooth with several sinusoidal Fourier components of similar amplitudes which removes the problem of small amplitudes of the Fourier components. In addition, the more detailed experimental analysis of TMDSC carried out in the present set of investigations has lead to some observations on procedures of measurement which are not sound when applied to TMDSC, although valid in the standard DSC procedure. Two of these are baseline-subtraction and data-smoothing in the time-domain before Fourier transformation. The reason for this complication is that in TMDSC with sawtooth modulation, time intervals are incorporated in the evaluation when the calorimeter is not in steady-state. Methods are indicated to alleviate these difficulties, specific to sawtooth modulation.

2. Computational details for sawtooth modulation

For temperature-modulation about the temperature T_0 with a centrosymmetric sawtooth, as carried out in quasi-isothermal TMDSC ($\langle q \rangle = 0$), one obtains the following series of harmonics

$$T(t) - T_0 = \frac{8A_{T_s}}{\pi^2}\left[\sin\omega t - \frac{1}{9}\sin 3\omega t + \frac{1}{25}\sin 5\omega t - \frac{1}{49}\sin 7\omega t + \frac{1}{81}\sin 9\omega t - \cdots\right], \quad (1)$$

where A_{T_s} is the modulation amplitude; ω, the basic frequency in rad s^{-1}; and t, the time. In order to generate a complex sawtooth $T_x(t)$ with equal amplitudes for four of the harmonics of the Fourier series of Eq. (1), one can add the following four series as shown

$$\begin{aligned}
T_1(t) &= \frac{8A_{T_s}}{\pi^2}\left[\sin\omega t - \frac{1}{9}\sin 3\omega t + \frac{1}{25}\sin 5\omega t - \frac{1}{49}\sin 7\omega t + \frac{1}{81}\sin 9\omega t - \cdots\right]\\
T_3(t) &= \frac{80A_{T_s}}{9\pi^2}\left[\sin 3\omega t - \frac{1}{9}\sin 9\omega t + \cdots\right]\\
T_5(t) &= \frac{192A_{T_s}}{25\pi^2}\left[\sin 5\omega t - \cdots\right]\\
T_7(t) &= \frac{400A_{T_s}}{49\pi^2}\left[\sin 7\omega t - \cdots\right]\\
\hline
T_x(t) &= \frac{8A_{T_s}}{\pi^2}\left[\sin\omega t + \sin 3\omega t + \sin 5\omega t + \sin 7\omega t - \frac{8}{81}\sin 9\omega t - \cdots\right].
\end{aligned} \quad (2)$$

The result is the complex series $T_x(t)$, illustrated in Fig. 1, together with its derivative, which has the appearance of a heat-flow rate and representing a meander of different amplitudes. This precise complex sawtooth has 26 different segments. The harmonics of

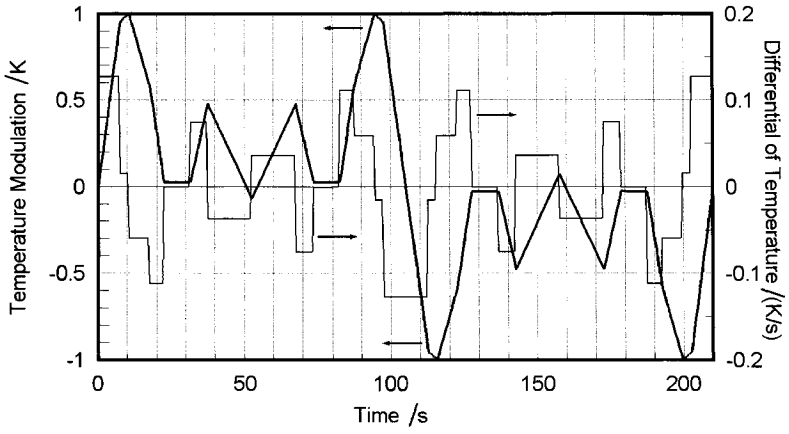

Fig. 1. Sample temperature $T_s(t)$ (heavy line, left ordinate) and its derivative $dT_s(t)/dt$ (thin line, right ordinate) as given by Eq. (2) for a modulation period p of 210 s.

$T_x(t)$ and $dT_x(t)/dt$ for the order of the harmonics, v=1, 3, 5, 7, and 9 and their sums are shown in Figs. 2 and 3. The harmonics of $T_x(t)$ with v=1, 3, 5, and 7 have the same amplitudes, the harmonic with v=9 is smaller. Higher harmonics are not shown in the figure, but rapidly decrease further with v>9. The temperature modulation $T_x(t)$ should, thus, provide an advantage over modulation with Eq. (1) for the calibration of the frequency dependence of the apparent heat capacity, developed earlier [7].

The calculation of the heat capacity, C_p, from the various harmonics requires the evaluation of the amplitudes of the heat-flow rate for each harmonic v, $A_{HF}(v)$, and the corresponding sample temperature, $A_{T_s}(v)$

$$C_p = \frac{A_{HF}(v)}{A_{T_s}(v)} \frac{1}{v \cdot \omega} \times K(v\omega), \tag{3}$$

where $K(v\omega)$ is a dimensionless constant, which is usually set approximately by comparison with the heat of fusion of indium, and later improved by measurement of C_p of sapphire as a calibrant.

In TMDSC under conditions of sinusoidal modulation which maintains steady state, $K(v\omega)$ in Eq. (3) is

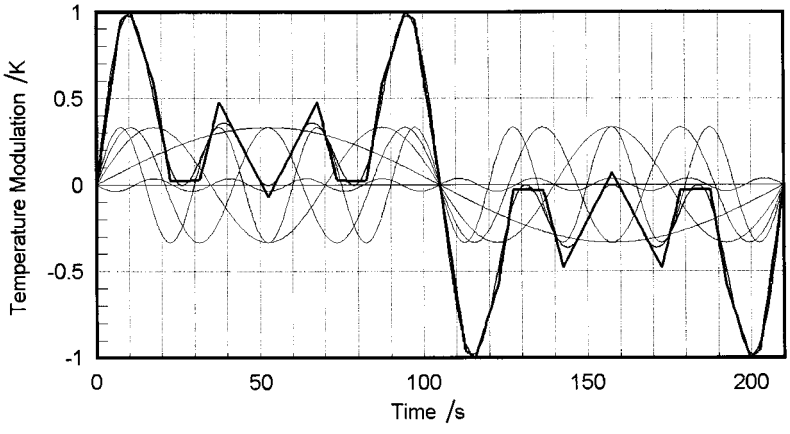

Fig. 2. Harmonics v=1, 3, 5, 7, and 9 of the sample temperature $T_s(t)$ (thin lines) and their sum (intermediate line) in comparison to the curve shown in Fig. 1 (heavy line).

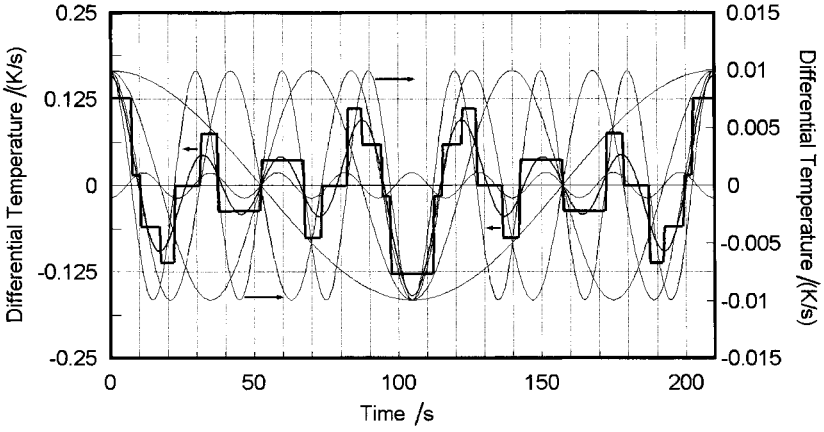

Fig. 3. Harmonics v=1, 3, 5, 7, and 9 of the derivative of the sample temperature $dT_s(t)/(vdt)$ (right ordinate, thin lines) and the sum of $dT_s(t)/dt$ (left ordinate, intermediate line) in comparison to the curve shown in Fig. 1 (heavy line).

given by $[1+(C_r\omega/K)^2]^{1/2}$. It derives from the necessity to correct the amplitude of the heat-flow rate for the different steady-state behaviors of the sample and reference calorimeters (C_r=heat capacity of the reference calorimeter, K=Newton's law constant) [8,9].

For sawtooth modulation, steady state is always lost immediately after each abrupt switch in steady state. As soon as the steady state is lost in modulated TMDSC, an additional dependency of $K(v\omega)$ develops, affected by sample and reference masses, type of sample, calorimeter positioning, and the involved thermal contacts. Although for the power-compensated DSC, it was suggested to correct the measured data by using the measured phase shift between the heating and heat-flow rates [10], a more correct method seems to be the use of the correction function:

$$K(v\omega) = \sqrt{1 + \tau^2(v\omega)^2}, \qquad (4)$$

where τ is the time-constant that depends on the instrument, reference and sample [6]. The time constant τ in Eq. (4) can be obtained by plotting the inverse of the squared, uncorrected heat capacity of Eq. (3) versus the square of the frequency [7]. The intercept of the plot at $(v\omega)^2=0$ is directly the inverse of the squared, true heat capacity if the heat-flow rate was calibrated before. Eq. (4) has by now been used successfully for empirical fitting of results from the Perkin-Elmer DDSC™ [11], the Mettler-Toledo ADSC™ [12,13], and the TA Instruments MDC™ [14]. For the latter this empirical fitting is only necessary if steady state is lost.

It should be noted that an additional calibration of the heat-flow rate must be done, as mentioned above, at every temperature by comparison with an identical measurement of a calibrant, such as sapphire. Both measurement and calibration runs must, naturally, also be baseline-corrected, which also causes small errors, as will be discussed below.

With the complex sawtooth of Eq. (2), a single experiment can produce the several measurements at different frequencies necessary to assure a statistically significant precision in the linear regression and extrapolation of Eq. (4) to $(v\omega)^2=0$. The application of Eq. (3) implies that the measured heat-flow rate is linearly related to the temperature change and that the superposition principle holds [15,16]. Linearity of the response requires an instrument which also responds linearly in the sum of all distortions of the output signal, which in case of the Perkin-Elmer DSC has been proven and represented by the Green's function (apparatus function) [17], although limits apply, as will be shown below in the discussion of baseline correction and instrumental problems.

The question may be raised (and has been asked by the reviewer) if modulation with any other simple, non-sinusoidal function may similarly be used to simultaneously produce multiple frequency excitation of the sample temperature and result in a heat-flow-rate response useable for the evaluation of Eq. (3) at

different frequencies. The sawtooth was not only chosen because of its multiple terms in the Fourier series of Eq. (1), but also because of the initial detriment of the rapid decrease in amplitude of the higher harmonics and the missing even harmonics which spaces the measured frequencies more widely. By the summation of Eq. (2), the detriment of decreasing amplitudes could be removed to such a degree, that the total temperature variation in (Fig. 2), shown by the heavy line, can be almost perfectly fitted by the sum of the first five harmonics (thin line), i.e., adding any higher harmonics cannot yield any more significant information, and all of the used harmonics have equal contributions to the sample temperature (except the smaller 9th harmonic).

It may be suggested that a meander profile, which consists of a constant temperature switched periodically by $\pm A_{T_s}$ about the temperature, T_0 is even easier to program. The Fourier series of this modulation is easily written for the case of crentrosymmetry as

$$T(t)-T_0=\frac{4A_{T_s}}{\pi^2}\left[\sin\omega t+\frac{1}{3}\sin 3\omega t-\frac{1}{5}\sin 5\omega t+\frac{1}{7}\sin 7\omega t-\frac{1}{9}\sin 9\omega t+\cdots\right]. \quad (5)$$

This is a series with linearly decreasing amplitudes, and thus much less suited for changing to equal amplitudes by the simple method employed here in Eq. (2). Furthermore, the meander is discontinuous at any time that is a multiple of $p/2$. Also, note that except for a phase shift of 90° and a different amplitude, Eq. (5) is the derivative of Eq. (1), and mathematically the differential heat-flow rate would become similar to the second derivative of Eq. (1), i.e., it would alternate between zero (at constant temperature) and $\pm\infty$ (at multiples of $p/2$). Only due to the inability of the calorimeter to reach instantaneous steady state in the vicinity of times equal to multiples of $p/2$ is then a measurement possible, which approaches, however, the appearance of a sawtooth, interrupted by isothermal segments. Such modulated temperature, however, is more complicated to model and usually does not exclude even harmonics. Trial and error would show if such simple modulation yields acceptable results, just as we could prove that a heat-flow DSC with rather poor sawtooth control produces useful multi-frequency modulation [14].

3. Simplified complex sawtooth for temperature modulation

The quality of the fit to the curves of Fig. 1 shows that the sum of harmonics represents the curves well. Since, however, this precise representation is not a condition for successful frequency-dependent TMDSC, the 26 segments were simplified to a complex sawtooth of only 14 segments. Table 1 gives an example for an overall period p of 210 s. Each subsegment is 15 s long and the harmonics with $v = 1$, 3, 5, and 7 correspond to the periods p of 210, 70, 42 and 30 s. The 9th harmonic with a period of $23\frac{1}{3}$ s is used for reference. It has a distinctly lower amplitude, but according to Eq. (2), its amplitude is still increased by a factor nine relative to a single sawtooth and has proven to be still useful for actual measurement [11–14].

The appearance of the approximate complex sawtooth $T_c(t)$ and its meander-like derivative $dT_c(t)/dt$ are shown in Fig. 4 and the analyses corresponding to Figs. 2 and 3 are displayed in Figs. 5 and 6. The amplitudes of the various harmonics are collected in Table 2. Overall, this complex sawtooth fulfills the need of a temperature program to analyze the frequency-dependence of the sample response to temperature modulation, as outlined above. Since it is a

Table 1
Approximate complex sawtooth program for $\omega = 210$ s[a]

Segment No.[b]	Time (s)	Change in temperature (K)
1	0→7.5	0.0→1.0
2	7.7→22.5	1.0→0.0
3	22.5→37.5	0.0→0.5
4	37.5→52.5	0.5→0.0
5	52.5→67.5	0.0→0.5
6	67.5→82.5	0.5→0.0
7	82.5→97.5	0.0→1.0
8	97.5→112.5	1.0→−1.0
9	112.5→127.5	−1.0→0.0
10	127.5→142.5	0.0→−0.5
11	142.5→157.5	−0.5→0.0
12	157.5→172.5	0.0→−0.5
13	172.5→187.5	−0.5→0.0
14	187.5→202.5	0.0→−1.0
15	202.5→210.0	−1.0→0.0

[a] Note that in order to keep a centrosymmetric sawtooth, segments 1 and 15 are half segments.

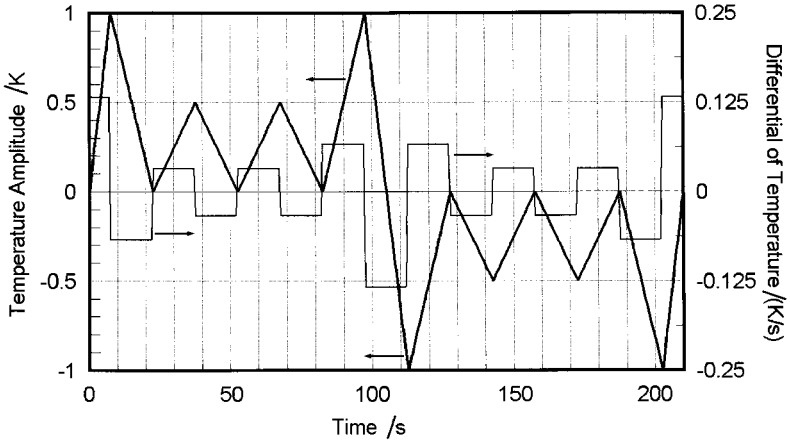

Fig. 4. Sample temperature $T_x(t)$ (heavy line, left ordinate) and its derivative $dT_x(t)/dt$ (thin line, right ordinate) for the complex sawtooth given in Table 1 for a modulation period p of 210 s.

Table 2
Amplitudes of the various harmonics[a]

Number of the harmonics (v)	Amplitude of T_x (K)	Amplitude of dT_x/dt (K s^{-1})	Amplitude $v\ dT_x/(v\ dt)$ (K s^{-1})[b]
1st	0.37819	0.011315	0.011315
(2nd)	(1.5×10^{-6})	(9.0×10^{-8})	(4.5×10^{-8})
3rd	0.25112	0.022538	0.007531
5th	0.21721	0.032487	0.006497
7th	0.34771	0.072790	0.010399
(9th)	(0.06711)	(0.018058)	(0.002644)

[a] For the complex sawtooth of Fig. 1, column 2 has the constant values 0.3325, and column 4 the constant value of 0.00995 for v=1, 3, 5 and 7; the second harmonic amplitudes are zero.

[b] These amplitudes are the normalized data of column 3 by division with v, the order of the harmonic.

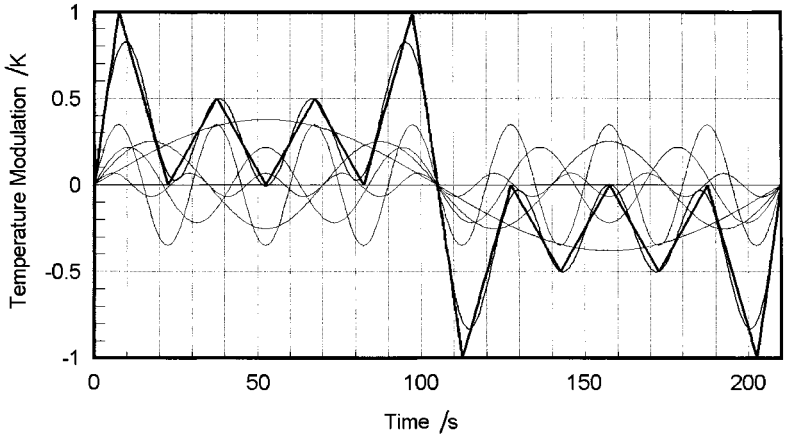

Fig. 5. Harmonics v=1, 3, 5, 7, and 9 of the sample temperature $T_x(t)$ (thin lines) and their sum (intermediate line) in comparison to the curve shown in Fig. 4 (heavy line).

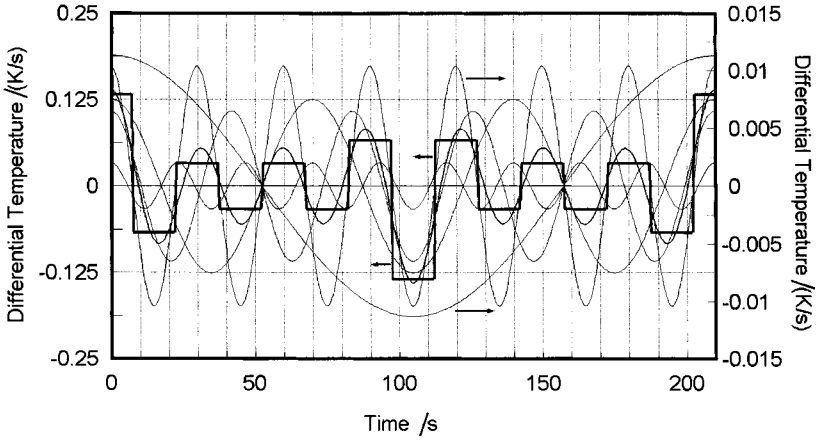

Fig. 6. Harmonics v=1, 3, 5, 7, and 9 of the derivative of the sample temperature $dT_x(t)/(vdt)$ (right ordinate, thin lines) and the sum of $dT_x(t)/dt$ (left ordinate, intermediate line) in comparison to the curve shown in Fig. 1 (heavy line).

single-run measurement, the analysis could be included in the software for data treatment, together with the extrapolation to zero frequency described in Ref. [7]. Furthermore, the 14 segments of the complex sawtooth are sufficiently simple to be programmed manually with any high-quality, standard DSC and repeated continually for quasi-isothermal TMDSC analysis. Characteristic of any TMDSC experiment is its Lissajous figure, consisting of a plot of the heat-flow rate (represented by the differential of temperature) versus the temperature modulation, as displayed in Fig. 7. Since all figures in this paper are derived by calculations based on the modeling software of [18] on the sawtooth described in Table 1, it excludes any instrument effects. Fig. 7 can, thus, used to be compared to any actual TMDSC runs and help in the interpretation of the results. The deviations from a perfect vertical on changing the heating rates in Fig. 7 are due to the resolution of only $\frac{1}{2}$ s in the spread-sheet used for analysis. In actual measurements one finds in these temperature regions the approach to steady state.

The absence of the even harmonics in the Fourier series shown in Table 2 is a measure of the centrosymmetric nature of the temperature modulation and the

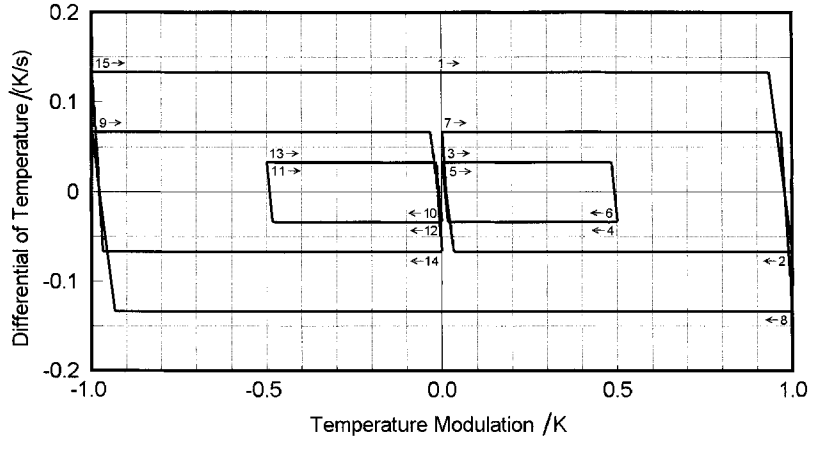

Fig. 7. Lissajous figure of the complex sawtooth of Fig. 4 consisting of a plot of $T_x(t)$ versus its derivative $dT_x(t)/dt$. The numbers and arrows in the figure indicate the segments and directions of progress in temperature of Table 1.

corresponding calorimetric response. The small residual second harmonic of Table 2 results from rounding errors. The spreadsheet employed for the analysis was described earlier [18] and can easily be expanded for the higher harmonics and off-line data evaluation.

For standard TMDSC with an underlying heating rate, $\langle q \rangle$, the required temperature change must be added to the sawtooth. As long as the to be measured heat capacity is independent of frequency and constant over the range of one modulation, the deconvolution of the added thermal effect due to $\langle q \rangle$ is a constant and can be used to get a measure of the heat capacity as derived from standard DSC [2–4]. If the heat capacity is frequency-dependent, the measured apparent heat capacity will contain contributions from a Doppler effect which is caused by superposition of the frequency ω and the linear heating rate $\langle q \rangle$. Details of this effect were worked out for the analysis of the glass transition [19].

4. Baseline correction and instrumental problems

All figures presented in this paper are idealized and do not include any instrument effects. As shown in Fig. 4, the complex sawtooth used for the discussion is perfect, as defined in Table 1. If this sawtooth is produced at the heater of the calorimeter as T_b, the sample temperature T_s lags behind T_b because of the sample heat capacity and the thermal resistance of the path of heat flow in the calorimeter. A calculation which considers these effects for two segments of the sawtooth is illustrated in Fig. 8. The calculation is based on the Fourier equation of heat flow, which is a linear differential equation [1]. The solutions before and after changing the heating rate at t_1 are listed in Fig. 8. Despite the lags, the different amplitudes of the Fourier harmonics of the temperature differences can be introduced into Eq. (3) and with the proper $K(v\omega)$ yield the correct heat capacities [20]. As long as the changes are linked by the Fourier equation, the two temperature differences are linearly coupled, as shown in Fig. 8, and the analysis of the TMDSC data yields the proper heat capacity even if steady state is lost, and even if steady state is never reached during the modulation periods. As soon as the response of the system is nonlinearly disturbed, as by software-dictated changes that cannot be described by linear differential

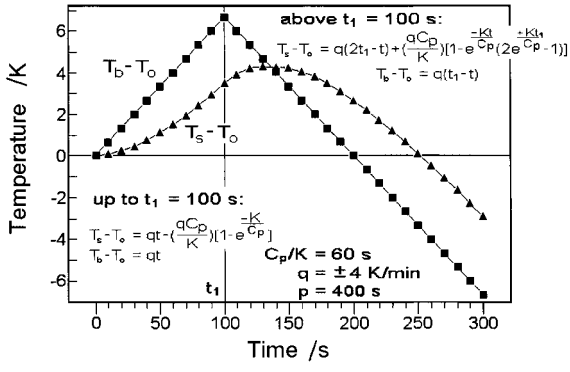

Fig. 8. The effect of heat capacity and thermal resistance on two segments of a sawtooth [16]. A perfect sawtooth is assumed as heater temperature T_b, the sample temperature T_s is computed as indicated. A similar calculation can be made for the reference temperature T_r. The value of C_p/K is chosen arbitrarily to illustrate an easily recognizable effect.

equations, Eq. (3) needs appropriate corrections, which are usually, however, not available to the experimenter and have to be deduced empirically.

Software problems of particular importance are spikes introduced in the heat flow at the time of changing heating rate at t_1 of Fig. 8. These spikes arise from the improper response of the calorimeter to the change in heater temperature. Although the spikes can sometimes be removed by subtracting a baseline run of two empty calorimeters in the time domain, it will be shown next, that this is not a fully valid correction method. Another method to remove the spikes and other noise of the recording is to smooth the calorimeter response over a number of data points. Again, such smoothing can destroy the linearity if it removes, e.g., exponential changes of the system as occur on approach to steady state and are shown in Fig. 8. The same effect is illustrated in more detail in the next two paragraphs on hand of problems with baseline subtraction. It should, however, be noted that the errors introduced by baseline subtraction and smoothing are often small and of concern only if a precision in heat capacity of better than $\pm 1\%$ is desired [13]. Not introducing these mathematically unfounded corrections usually causes a much bigger error, so that the only route to precision calorimetry is to minimize such problems by choosing proper instrumental conditions. Recognizing these problems of TMDSC may also induce the development of new, improved calorimeters by the instrument providers.

As just mentioned, for a measurement of the true heat capacity by TMDSC it is not only necessary to complete runs at different frequency for the sample and the calibrant, as outlined above, but both of these experiments must also be corrected for the asymmetry that may exist between the reference and sample calorimeter. Two methods are commonly used for this correction. One involves a complete third run to establish the heat-capacity correction using Eq. (3) as follows: two empty pans are measured against each other in a baseline run and evaluated in the same fashion as the sample and reference runs. Basically this method is correct, but a problem arising in this method is that positive and negative asymmetries yield the same positive amplitudes. Methods have been developed to overcome these difficulties by introduction of an artificial asymmetry of known direction, or by actual evaluation of the phase shift of the baseline run [21].

Another method, which is mathematically not sound for TMDSC, was adapted from the routine measurements by standard DSC where it is a proper method since the subtraction is only carried out under condition of steady state. It requires to establish a baseline by running the calorimeter with two empty pans and subtracting it from the reference and sample runs in the time domain (before Fourier transformation to the frequency domain, i.e., computation of the amplitudes of modulation). Several manufacturers include an automatic subtraction of this baseline in order to facilitate the measurements. For quantitative measurements of high quality, we observed that this method is basically flawed, although the error may be partially compensating between the sample and reference runs, and at least at present be of similar magnitude as the errors introduced by defects in the instruments and operating systems.

To illustrate the problem of the method of baseline subtraction in the time domain, Table 3 shows data for two runs and the effect of subtraction of the runs in the time domain followed by analysis, as indicated in the footnote and explained in more detail in [20]. The calculations were done by assuming no instrument effects and strict adherence to the Fourier equation of heat flow for the computation of the temperature lags, as illustrated also in Fig. 8. In the first two rows of Table 3 it is shown that despite reaching steady state only in the data of File No. 4, both Files No. 4 and No. 6 can after proper correction give precise heat capacities [20]. Subtracting Files No. 4 as an assumed baseline run from the sample run of File No. 6 in the time domain, followed by the standard TMDSC analysis leads, however, to an error of −1.5%, as is shown in the last row of Table 3. Despite linearity of all calculations, the time-dependent heat flows of the sample run (No. 6) and the baseline run (No. 4) are not additive for the Fourier analysis since they contain contributions from the exponential approaches to steady state which are different for reference and sample.

5. Conclusions

It is shown that one can generate a complex sawtooth that may permit measurement of an apparent

Table 3
Results of the calculation of heat capacity for sawtooth modulation[a]

File No.	$C_s - C_r$ (K)	A_Δ/A (ω)	Deviation (%)	Corrected	Deviation (%)
4	3−1=2	1.996	−0.20	2.00	0
6	60–1=59	58.886	−0.19	59.00	0
6–4	59−2=57	56.015	−1.73	56.126	−1.5

[a]The heat capacities C_s and C_r, when divided by the Newton's Law constant K, are given in seconds, s; the linear heating and cooling rates of the sawtooth q are 0.04 K s^{-1}; A, the amplitude set for the sawtooth is ±1.0 K; the period p is 100 s; the frequency $\omega=2\pi/p=0.062832$ rad s^{-1}; at time $t=0$: $T_s=T_r=T_o$; $C_p(\text{TMDSC})/K=(A_\Delta/A)/\omega$; the correction factor for the TMDSC heat capacity is $[1+(C_r\omega/K)^2]^{1/2}$ [see Eq. (4)]. The Sample temperature during the heating or cooling cycle is (subscripts: sample=s, reference=r): $T^1_{s,r} = T_{s,r}(t_x) \pm q(t - t_x) \mp (qC_{s,r}/K)[1 - \exp(-K(t - t_x)/C_{s,r})]$. The approach to steady state after the switch from heating to cooling and vice versa (at $t=t_x$) is: $T^2_{s,r} = (\pm A \mp T_{s,r}(t_x))[1 - \exp(-K(t - t_x)/C_{s,r})]$, where T^1 and T^2 are the appropriate solutions of the heat-flow rate equation, as given in [1], see also Fig. 8. The total response to the sawtooth modulation is, thus: $T_{s,r}(t) = T^1_{s,r}(t) + T^2_{s,r}(t)$. The deviations in the last column are computed relative to the correct values of column 2.

heat capacity as a function of frequency to eliminate instrument effects. It may even be possible after subtraction of the instrument effects to establish the frequency dependence of heat capacity as it is of interest in characterizing glass transitions [5]. In a series of subsequent papers, modulation with this complex sawtooth will be described, analyzed, and discussed based on data from a power-compensated DSC and two heat-flux DSCs [11–14]. In the course of the study of sawtooth modulation, it was also discovered that software effects, data smoothing, and the common baseline subtraction in the time domain, are not mathematically sound for the use in TMDSC. It is hoped that future instrument developments take these observations into consideration to advance the quality and capability of TMDSC.

Acknowledgements

This work was supported by the Division of Materials Research, National Science Foundation, Polymers Program, Grant No. DMR-9703692 and the Division of Materials Sciences, Office of Basic Energy Sciences, US Department of Energy at Oak Ridge National Laboratory, managed by Lockheed Martin Energy Research Corp. for the U.S. Department of Energy, under contract number DE-AC05-96OR22464.

References

[1] B. Wunderlich, Thermal Analysis, Academic Press, New York, 1990 (For an update in form of the computer-course Thermal Analysis of Materials 1999, see our web-site, found at the URL: http://web.utk.edu/athas.)

[2] M. Reading, B.K. Hahn, B.S. Crowe, Method and Apparatus for Modulated Differential Analysis, 6 July 1993, US Patent 5 224 775.

[3] P.S. Gill, S.R. Sauerbrunn, M. Reading, J. Thermal Anal. 40 (1993) 931.

[4] M. Reading, A. Luget, R. Wilson, Thermochim. Acta 138 (1994) 295.

[5] B. Wunderlich, I. Okazaki, Temperature-modulated calorimetry of the frequency dependence of the glass transition of poly(ethylene terephthalate) and polystyrene, in: M.R. Tant, A.J. Hill (Eds.), Structure and Properties of Glassy Polymers, ACS Symposium Series, 710 (1998) 103, Am. Chem. Soc., Washington, DC.

[6] R. Androsch, I. Moon, S. Kreitmeier, B. Wunderlich, Thermochim. Acta (still not publised), in press.

[7] R. Androsch, B. Wunderlich, Thermochim. Acta 333 (1999) 27.

[8] B. Wunderlich, Y. Jin, A. Boller, Thermochim. Acta 238 (1994) 277.

[9] A. Boller, Y. Jin, B. Wunderlich, J. Thermal Anal. 42 (1994) 307.

[10] J.E.K. Schawe, Thermochim. Acta 298 (1997).

[11] Y.K. Kwon, R. Androsch, M. Pyda, B. Wunderlich, Thermochim. Acta (1999), submitted for publication.

[12] I. Moon, R. Androsch, B. Wunderlich, Thermochim. Acta (1999), accepted for publication.

[13] J. Pak, B. Wunderlich, Thermochim. Acta (1999), submitted for publication.

[14] M. Pyda, Y.K. Kwon, B. Wunderlich, Thermochim. Acta (1999), submitted.

[15] A. Hensel, C. Schick, Thermochim. Acta 304/305 (1997) 229.

[16] T. Ozawa, K. Kanari, Thermochim. Acta 253 (1995) 183.

[17] G.W.H. Höhne, J.E.K. Schawe, Thermochim. Acta 229 (1993) 27.

[18] B. Wunderlich, J. Thermal. Anal. 48 (1997) 207.

[19] L.C. Thomas, A. Boller, I. Okazaki, B. Wunderlich, Thermochim. Acta 291 (1997) 85.

[20] B. Wunderlich, A. Boller, I. Okazaki, K. Ishikiriyama, W. Chen, M. Pyda, J. Pak, I. Moon, R. Androsch, Thermochim. Acta 330 (1999) 21.

[21] K. Ishikiriyama, B. Wunderlich, J. Thermal Anal. 50 (1997) 337.